Results in Chemistry 7 (2024) 101277

Contents lists available at ScienceDirect

Results in Chemistry

journal homepage: www.sciencedirect.com/journal/results-in-chemistry

A novel Cadmium metal-organic framework with exceptional nonlinear optical properties: Unveiling anisotropic charge transport and optical limiting behavior

Anaglit Catherine Paul [a], Madhukar Hemamalini [a,*], Mohd Mustaqim Rosli [b], Savaridassan Jose Kavitha [a], Venkatachalam Rajakannan [c], V. Anbazhagan [d], David Stephen Arputharaj [e], Abdullah G. Al-sehemi [f,g], Kasthuri Balasubramani [h], Dian Alwani Zainuri [b,*], Ibrahim Abdul Razak [b,*]

[a] Department of Chemistry, Mother Teresa Women's University, Kodaikanal 624101, Tamil Nadu, India
[b] School of Physics, Universiti Sains Malaysia 11800, USM, Penang, Malaysia
[c] Centre of Advanced Study in Crystallography & Biophysics, University of Madras, Chennai 600085, Tamil Nadu, India
[d] Department of Chemistry, Vinayaka Mission's Kirupananda Arts & Science College, Vinayaka Mission's Research Foundation Deemed to be University, Salem 636308, Tamil Nadu, India
[e] Department of Physics, PSG College of Arts & Science, Coimbatore 641014, India
[f] Research Centre for Advances Materials Science (RCAMS), King Khalid University, Abha 61413, Saudi Arabia
[g] Department of Chemistry, College of Science, King Khalid University, Abha 61413, Saudi Arabia
[h] Department of Chemistry, Dr. Kalaingar Government Arts College, Kulithalai 639120, Tamil Nadu, India

ARTICLE INFO

Keywords:
Non-Centrosymmetric
Cadmium Metal-Organic Framework (Cd-MOF)
Band Structure Calculations
Optical Limiting

ABSTRACT

A novel non-centrosymmetric Cadmium Metal-Organic Framework (Cd-MOF) crystal with chemical formula $CdC_8N_8H_{14}O_2S_4$ was synthesized and characterized. The band structure and optical limiting properties of the Cd-MOF were investigated using Band structure calculations and Optical limiting studies. The band structure analysis showed that the crystal displayed a larger, highly dispersive band, highlighting significant anisotropic n-channel charge carrier mobility. The optical limiting study demonstrated that the Cd-MOF exhibited Reverse Saturable Absorption (RSA) behaviour with an optical limiting threshold value of 1094 kW/cm^2. The NLO behaviour of the Cd-MOF provides a promising potential for its application in NLO devices.

Introduction

The synthesis and structural characterization of Metal-Organic Frameworks (MOFs) remain an active area of research due to their extensive material and biological applications. MOFs are crystalline network materials constructed from metal nodes and organic linkers through robust coordination bonds [1–3]. They are typically synthesized using inorganic metal ions and organic linkers [4]. In this work, thiocyanate serves as a linker, bridging metal and organic ligands. In recent years, there has been a growing interest in MOFs due to their potential applications in various fields such as biotechnology, gas storage devices, medicinal chemistry, catalysis, biosensors, luminescent materials, drug-molecular recognition, industrial applications, agriculture, and synthetic chemistry [5–7]. 1,2,3-Triazoles are privileged nitrogen heterocyclic motifs with promising medicinal activities. They possess strong binding interactions with suitable molecular targets and exhibit favourable biological profiles [8]. Most triazole derivatives are commonly synthesized through the Copper(I)-catalyzed (CuAAC) 1,3-dipolar *cyclo*-addition reaction between azide and alkyne, as reported by Sharpless and co-workers [9]. Cadmium thiocyanate adducts of organic ligands represent an important class of compounds for the design and preparation of metal–organic frameworks [10]. Several Cadmium(II) thiocyanate complex adducts of monodentate organic ligands, such as methyl-substituted pyridines [11,12], dibenzylamine [13], dimethyl sulfoxide (DMSO) [14], and 4-chloropyridine [15], have been reported in the literature. Thiocyanate is an ambidentate ion capable of coordinating with metal ions via its S or N atoms. It can also bridge metal ions by employing both N and S atoms for coordination.

* Corresponding authors.
E-mail addresses: hemamalini2k3@yahoo.com (M. Hemamalini), dianalwani@usm.my (D. Alwani Zainuri), arazaki@usm.my (I. Abdul Razak).

https://doi.org/10.1016/j.rechem.2023.101277
Received 27 November 2023; Accepted 20 December 2023
Available online 23 December 2023

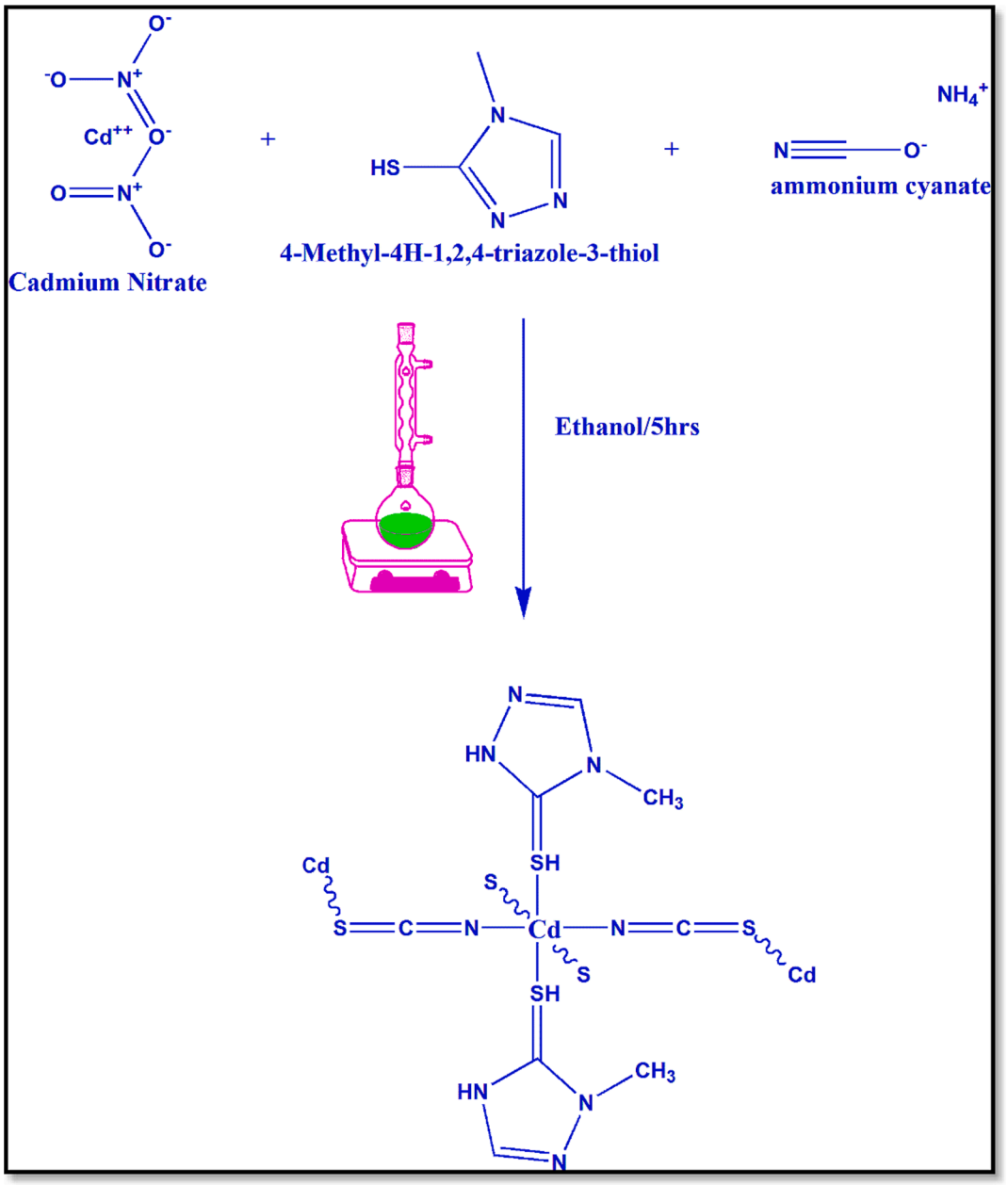
Cadmium Nitrate
4-Methyl-4H-1,2,4-triazole-3-thiol
ammonium cyanate
Ethanol/5hrs

Scheme 1.

Table 1
Experimental details.

Crystal Data	
Chemical Formula	$C_8H_{14}CdN_8O_2S_4$
Molecular Weight	494.91
Crystal system, space group	Monoclinic, P21/c
Temperature (K)	296
a, b, c (Å)	5.959 (3), 12.655 (6), 12.205 (5)
β (°)	112.359 (18)
V (Å3)	851.2 (7)
Z	2
Radiation type	Mo Kα
μ (mm^{-1})	1.79
Crystal size (mm)	0.59 × 0.21 × 0.16
Data Collection	
Diffractometer	BrukerAPEX-II CCD
Absorption correction	Multi-scan SADABS2014/5
Tmin, Tmax	0.220, 0.434
No. of measured, independent and observed [I> 2σ(I)] reflections	34,937, 2776, 2052
Rint	0.089
(sin θ/λ)max (Å−1)	0.734
Refinement	
R[F2 > 2σ(F2)], wR(F2), S	0.035, 0.091, 1.03
No. of reflections	2776
No. of parameters	111
H-atom treatment	H atoms treated by a mixture of independent and constrained refinement
Δρmax, Δρmin (e Å−3)	0.99, −0.88
CCDC No	2,221,312

The crystal structures of doubly bridged Cu(II) [16,17], Mn(II) [18], Ag (I) [19], and Cd(II) [20] complexes are known.

MOFs with π-conjugated electronic systems exhibit third-order nonlinear optics (NLO), showcasing potential applications in optical limiting (OL), optical switching, and mode-locked laser systems, etc [21–23]. Nonlinear optical (NLO) materials have garnered significant attention in optoelectronics applications. Metal-organic frameworks play a crucial role due to their exceptional nonlinear efficiency, transparency over the entire UV–visible region, and strong thermal and mechanical stability. Our research focuses on investigating the metal–organic framework of Cadmium (II) thiocyanate triazole complexes. To this end, we present the crystal structure and linear and nonlinear optical properties of Cd(II)-MOFs. The band structure and optical limiting properties of the Cd-MOF were elucidated through band structure calculations and optical limiting experiments.

Experimental

Synthesis and crystallization

A solution of NH_4NCS (76.1 mg in 5 ml of water) was mixed with an aqueous solution of cadmium nitrate [$Cd(NO_3)_2{\cdot}4H_2O$, 77.10 mg in 10 ml of water). The mixture was stirred for 30 min. This reaction mixture was gradually supplemented with the ligand 4-methyl-4H-1,2,4-tirazole-3-thiol (55.10 mg in 20 ml of ethanol). After five hours of refluxing, the resulting solution was filtered. After a few days, the filtrate yielded pale red crystals of (I) (Scheme 1) as the solvent slowly evaporated.

X-ray structure determination

The crystal was obtained by slow evaporation technique and which colourless crystal has a size of 0.587x0.214x0.156 mm. Assist of Bruker SMART APEXII CCD [24], area detector diffractometer had been collected XRD data into 293 K and with help of MoKα (λ = 0.71073 Å) radiation. The crystal data was solved using the direct method in SHELXS [25], refined using the full-matrix least-squares method in SHELXL [26]and all non-hydrogen atoms were refine anisotropic thermal parameters. The position of hydrogen was fixed riding atoms model to identifying high-resolution data. For the preparation of publication material, we had used programs such as WinGX [27], PLATON [28], ORTEP III [29], and which computed the crystallographic data (Table 1) was tabulated.

Uv–vis & spectrofluroimeter

Absorption spectra were captured using a JASCO V-750 UV–Vis spectrophotometer. In different solvents, sample is dissolved. A JASCO FP-8300 spectrofluorimeter was used to detect the fluorescence [30]. In phosphate buffered solution at pH 7.4, the excitation and emission maxima of NB are 636 nm and 669 nm, respectively. The samples were degassed in quarts cells (4 × 1 × 1) with high vacuum stopcocks for 15 min using only pure nitrogen gas.

Z-scan

Z-scan is one of the most effective methods for determining NLO characteristics [31]. The experiment setup is shown in Fig. 1. The setup of Z-scan with further details was described in [32]. Cd(II)-MOFs sample was dissolved in dimethyl sulfoxide (DMSO) at a concentration of 0.1 mM. All tests of the nonlinear optical measurements including nonlinear refractive index (n_2), nonlinear absorption coefficient (β) and third order susceptibilities (χ3), were performed with a silicon-amplified photodetector (PDA55) and a diode-pumped solid-state (DPSS) laser (Coherent Verdi-V5) operating at 637 nm continuous wave.

The thermal component leads in the calculation of the NLO since a CW laser is used. Consequently, the Thermal Lensing Model (TLM), a useful equation for NLR fitting, has considered the thermal effect (Equation (1).

NLR fitting (Equation (1).

$$T(z) = 1 - \frac{8\pi n_2 I_0 L_{eff} \frac{z^2_r}{w}}{1 + \frac{z^2}{z^2_r}\left(9 + \frac{z^2}{z^2_r}\right)} \tag{1}$$

Where,

The experimental results were then entered into equation (1) to determine the value of n_2.

The β, is estimated using the open-aperture Z-scan data. The equation [34] is given by

$$T(z, s = 1) = \sum_{m=0}^{\infty} \frac{[-q_0(z)]^m}{(m+1)^{3/2}} \tag{2}$$

where,

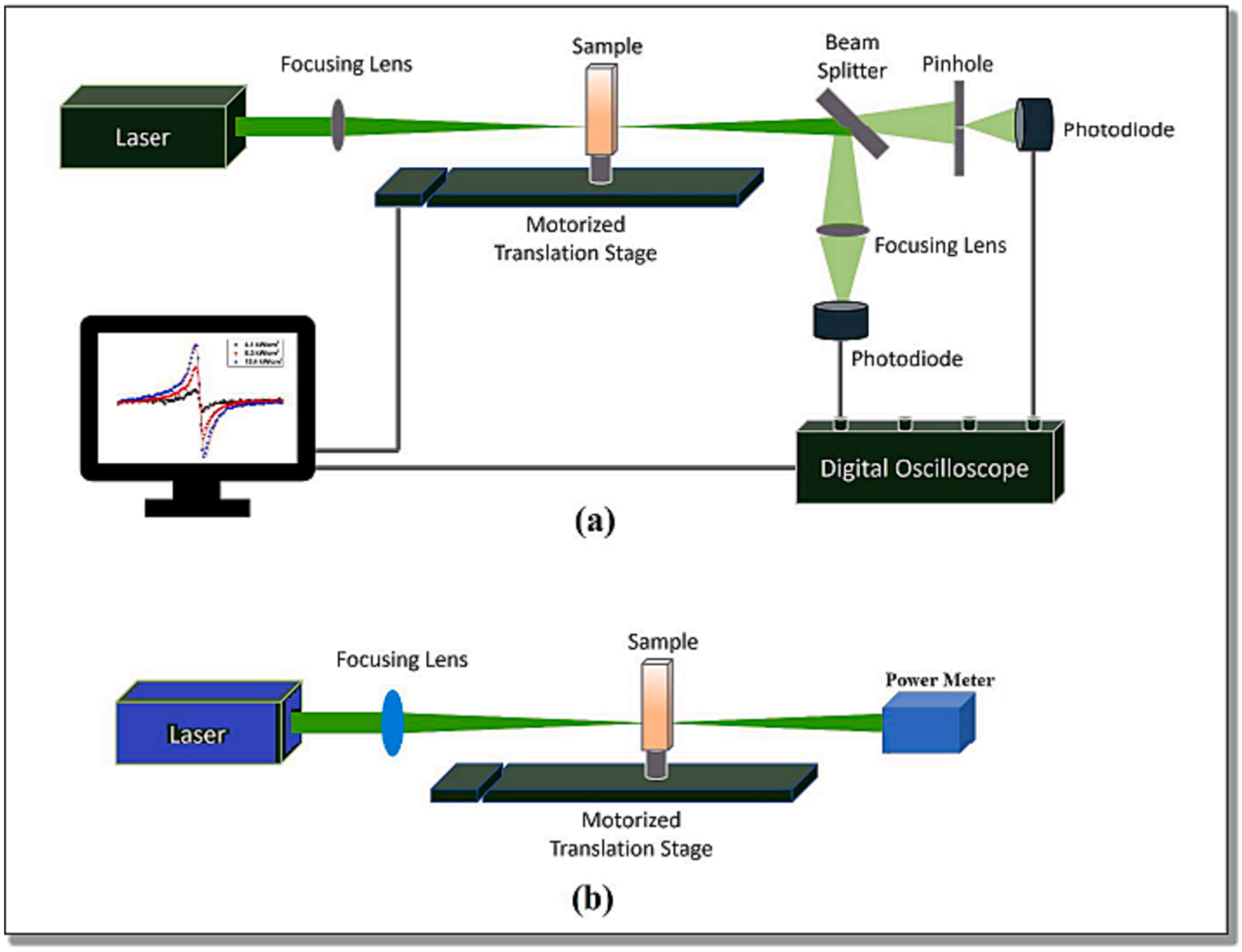

Fig. 1. (a) Open and closed Z-scan and Optical Limiting approach setup (b) shows the optical limiting setup.

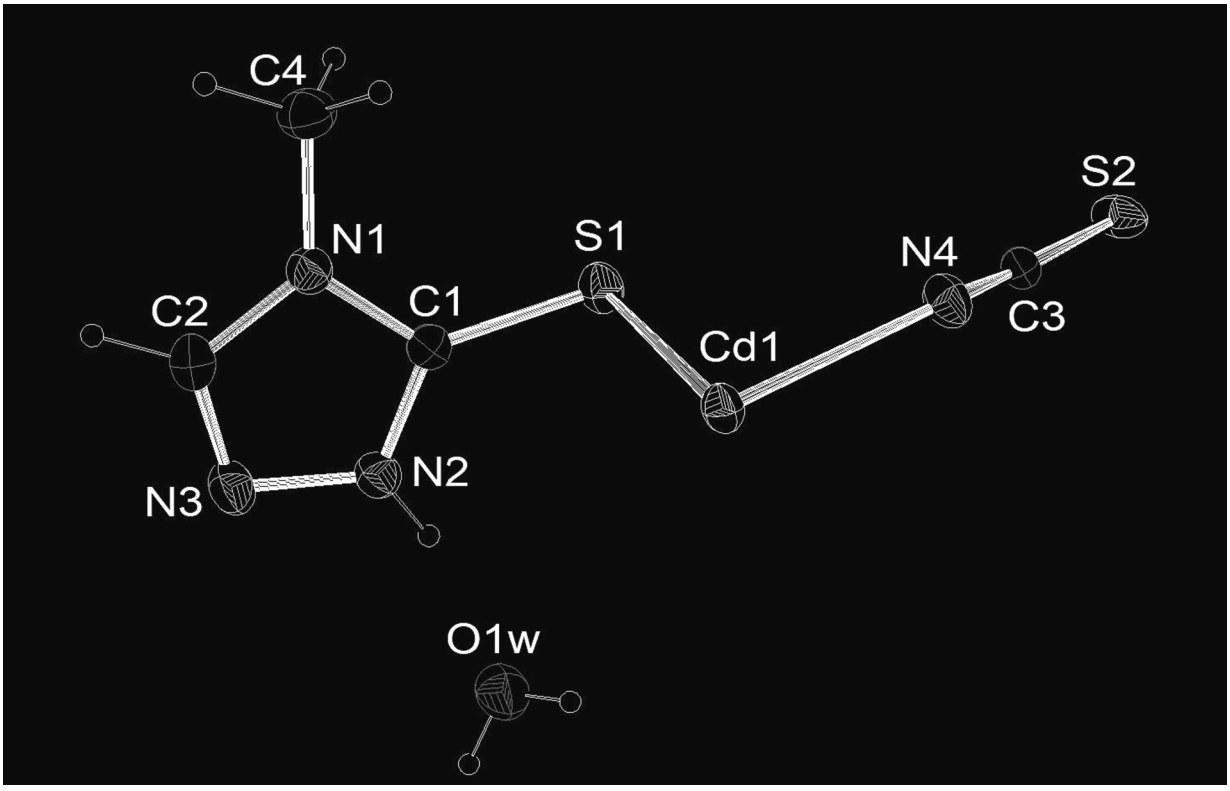

Fig. 2. ORTEP view of (I), showing 30% probability displacement ellipsoids plot.

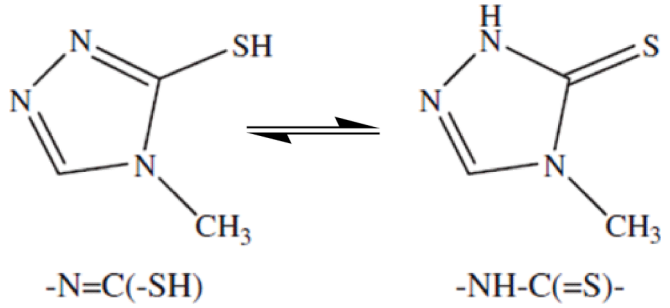

Scheme 2. .

$q_0(z) = \frac{\beta I_0 L_{eff}}{1+z2/ZR2}$,

$z_R = k\omega 02/2$= Beam diffraction length.
ω_0 = beam waist radius at the focal point.
$k = 2\pi/\lambda$ = Wave vector.

The formula of β is [33],

$$\beta = \frac{2\sqrt{2\Delta T_{p-v}}}{I_0 L_{eff}} \tag{3}$$

where,

λ = laser wavelength.
I_0 = Intensity of the laser beam at focus $z = 0$,

$$L_{eff} = \frac{[1 - exp(-\alpha L)]}{\alpha} \tag{4}$$

where,

L_{eff} = Effective thickness of the sample.
α = Linear absorption coefficient.
L = Thickness of the sample.

The n_2 and β are used to calculate the real $Re\chi^{(3)}(esu)$ and imaginary $Im\chi^{(3)}$ parts of the $\chi^{(3)}$,respectively. The definition of the relations [34,35] is as follows:

$$Re\chi^{(3)}(esu) = 10^{-4}\frac{\varepsilon_0 c^2 {n_0}^2}{\pi} n_2 \quad \left(\frac{cm^2}{W}\right) \tag{5}$$

and

$$Im\chi^{(3)}(esu) = 10^{-2}\frac{\varepsilon_0 c^2 {n_0}^2 \lambda}{4\pi^2}\beta\left(\frac{cm}{W}\right) \tag{6}$$

$$\left|\chi^3\right| = \left[\left((R_e(\chi^3))\right)^2 + \left(I_m(\chi^3)\right)^2\right]^{1/2} \tag{7}$$

where,

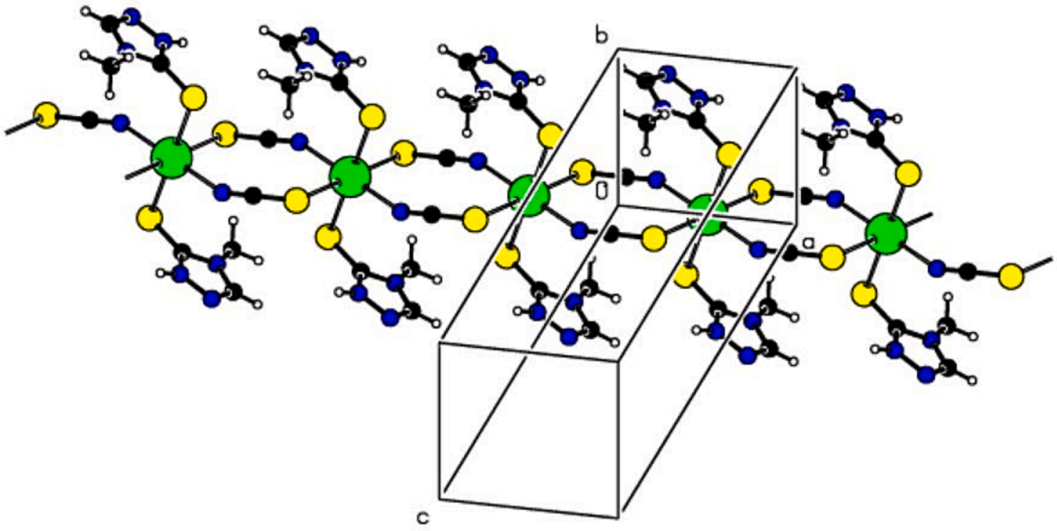

(a)

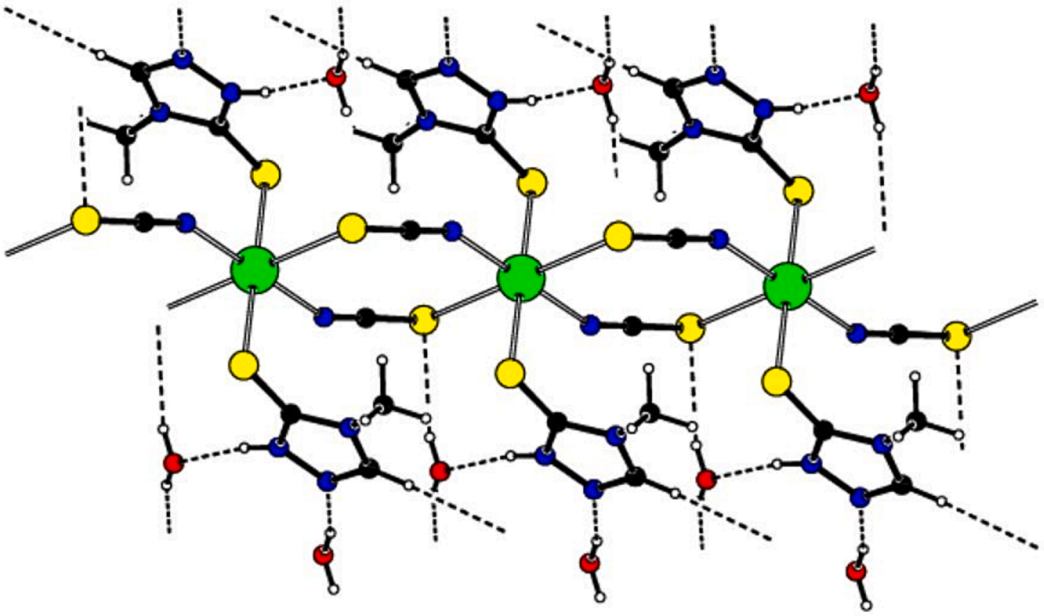

(b)

Fig. 3. (a) Polymeric network of Cd(II)-MOFs and (b) N—H···O & O—H···S intermolecular hydrogen bonding of (I).

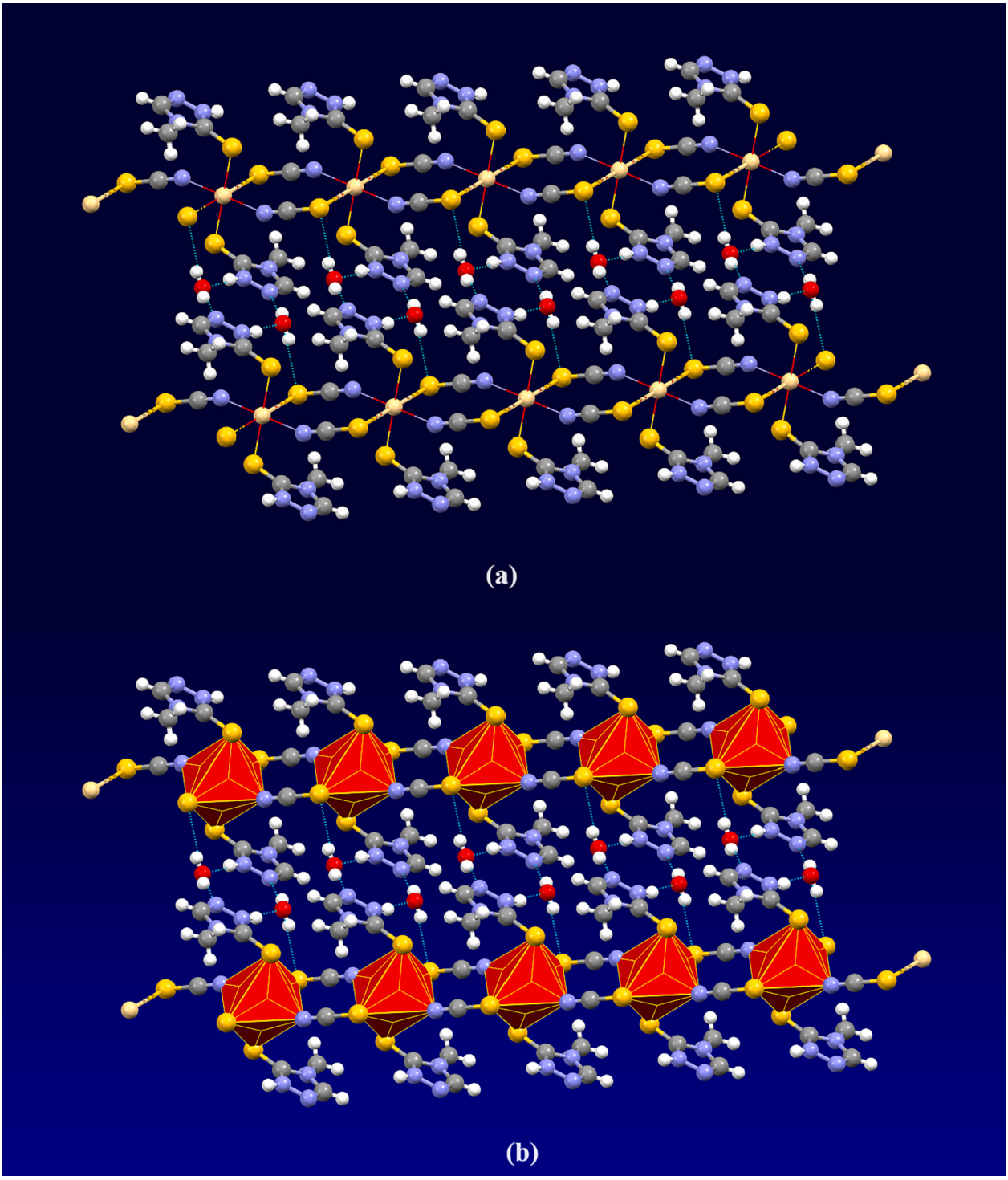

Fig. 4. Packing diagram of (I) (a) Coordination geometry of Cd (II) (b) polyhedral representation around the Cd(II) atom.

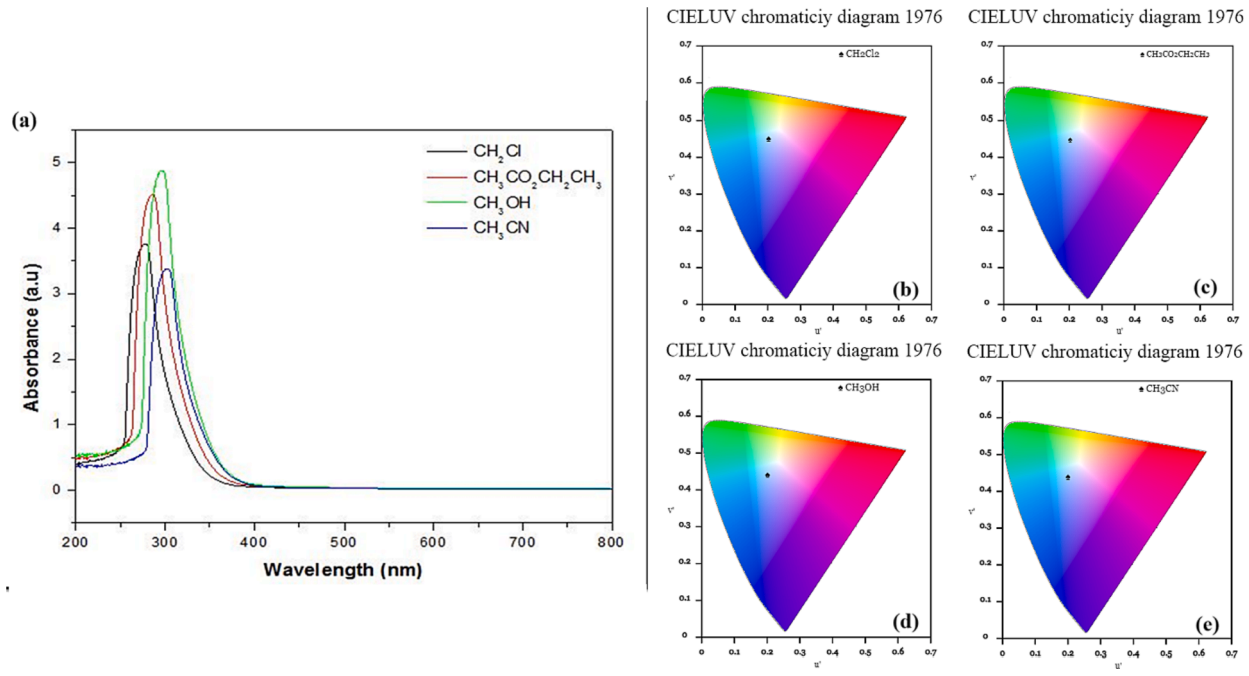

Fig. 5. (a) UV–visible absorption spectrum of Cd(II)-MOFs in CH_2Cl_2, CH3CO2CH2CH3, CH_3OH and CH_3CN Figure (b) (c) (d) (e) shows the chromocity diagram 1976 of the different solvents.

Table 2
Polarity index and wavelength of solvents.

S. No	Name of the solvent	Polarity Index	Wavelength (nm)
1	CH_2Cl_2	3.1	277
2	CH3CO2CH2CH3	4.4	285
3	CH_3OH	5.1	294
4	CH_3CN	5.8	302

ε_0 = Vacuum permittivity,
c = Light velocity in vacuum.

Optical limiting

Fig. 1(b) shows the optical limiting setup for investigated compound. The sample inside quartz cuvette with same concentration of 0.1 mM is placed perpendicularly. A laser diode and focusing lens are used in the setup to direct the laser beam toward the target sample. The convex lens

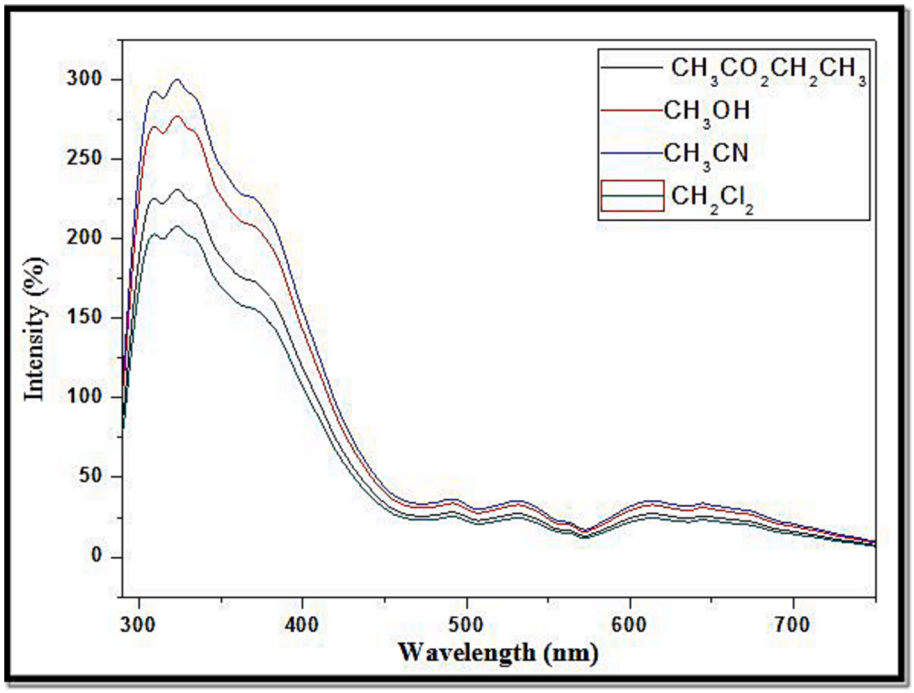

Fig. 6. (a) Photoluminescence spectrum of Cd(II)-MOFs in CH_2Cl_2, CH3CO2CH2CH3, CH_3OH and CH_3CN.

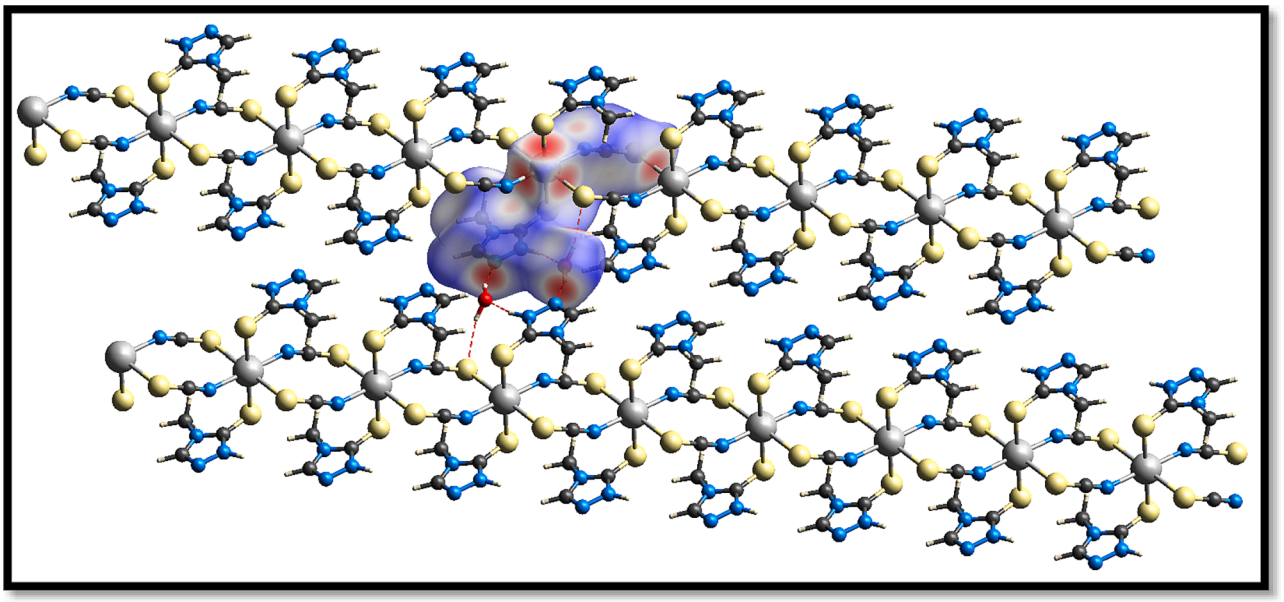

Fig. 7. HS mapped over d_{norm} of (I).

with a 25 mm focal length is used to gather the light signal generated by the sample and collimate it into the photodiode. The input power is changed between 1.4 and 1.9 mW.

Band structure and TDOS

Band structure and TDOS (Total Density of States) analyses [Fig. 12] were conducted using density functional theory (DFT) calculations performed with the Vienna ab initio simulation package (VASP) software [36,37]. These calculations employed the generalized gradient approximation (GGA) [38,39] of Perdew–Burke–Ernzerhof (PBE). The electronic wave functions were expanded using project augmented wave (PAW) methods [40], with a plane wave cutoff energy of 500 eV.

Results and discussion

X-ray structure analysis

The asymmetric unit contains one 4-methyl-4H-1,2,4-triazolinium-3-thiolate, a thiocyanate ion, a water molecule, and a cadmium ion (Fig. 2). The cadmium ions are symmetrically doubly bridged by thiocyanate ions and organic molecules, leading to a polymeric chain motif. This kind of metal–organic framework is also observed in bis-ethylene thiourea cadmium(II)thiocyanate and *catena*-poly[[diaqua cadmium (II)]-di-m-thiocyanato]- bis(2-amino-4,6 dimethylpyrimidine)][41]. In compound (I), the distorted octahedral coordination geometry of cadmium is completed by a pair of inversion-related thiocyanate and organic molecules. Here, the water molecule is directly not involved in the coordination geometry although it participates in non-covalent interactions between water and metal organic frameworks. The bond distances [Cd-N4 = 2.291 (3) Å, Cd-S = 2.5896 (12)Å] agree with those reported in the literature [42]. The thiocyanate ligands are almost linear [(NC– S) = 177.4, (3)] with sp hybridized carbon. The 4-methyl-4H-1,2,4-triazole-3-thiol molecule, tautomerism occurs with the thiol group and the neighboring nitrogen atom [-N = C(-SH) ↔ –NH-C(=S)-] (Scheme 2). A similar type of tautomerism is also observed in the crystal structure of Palladium(II) complexes with 1,2,4-triazole derivatives [43].

In the crystal structure of (I) there are no π…π and C—H…π interactions between the triazole

rings and metal coordination, and only intra and intermolecular O—H···N, O—H···S, N— H···O and weak C—H···O hydrogen bonds and metal coordination bonds are effective in the stabilization of the crystal structure (Fig. 3a & 3b). The formation of the 2-D supramolecular assembly is shown in Fig. 4a & 4b. The intermolecular charge transfer between the donor and acceptor groups of the molecules will be improved by the molecular packing patterns as seen in Figs. 3 and 4. The most crucial factor in establishing the hyper polarizability β values is the push–pull interactions between the electron withdrawing and electron donor groups [44,45].

UV–Vis spectra analysis

UV–Vis optical absorption spectra of Cd(II)-MOFs sample is measured in 4 solvents of varied polarity index (3.1–5.8) and the CIE chromocity plots of different solvent environment as shown in Fig. 5 (a-e). While changing solvents with polarity, CH_2Cl_2 (PI = 2.2), CH3CO2CH2CH3, (PI = 4.4), CH_3OH (PI = 5.1) and CH_3CN (PI = 5.8), shows a steady red shift upto 25 nm (Table 2).The red shift is observed with increased value of polarity index of the solvents. This behavior is due to electronic excitation can be associated with an increase in molecular dipole moment [46]. There is observable wavelength shift occurred as per solvent which is evident for the maximal absorption attributed to the aromatic ligand centred π-π* transitions [47]. At the

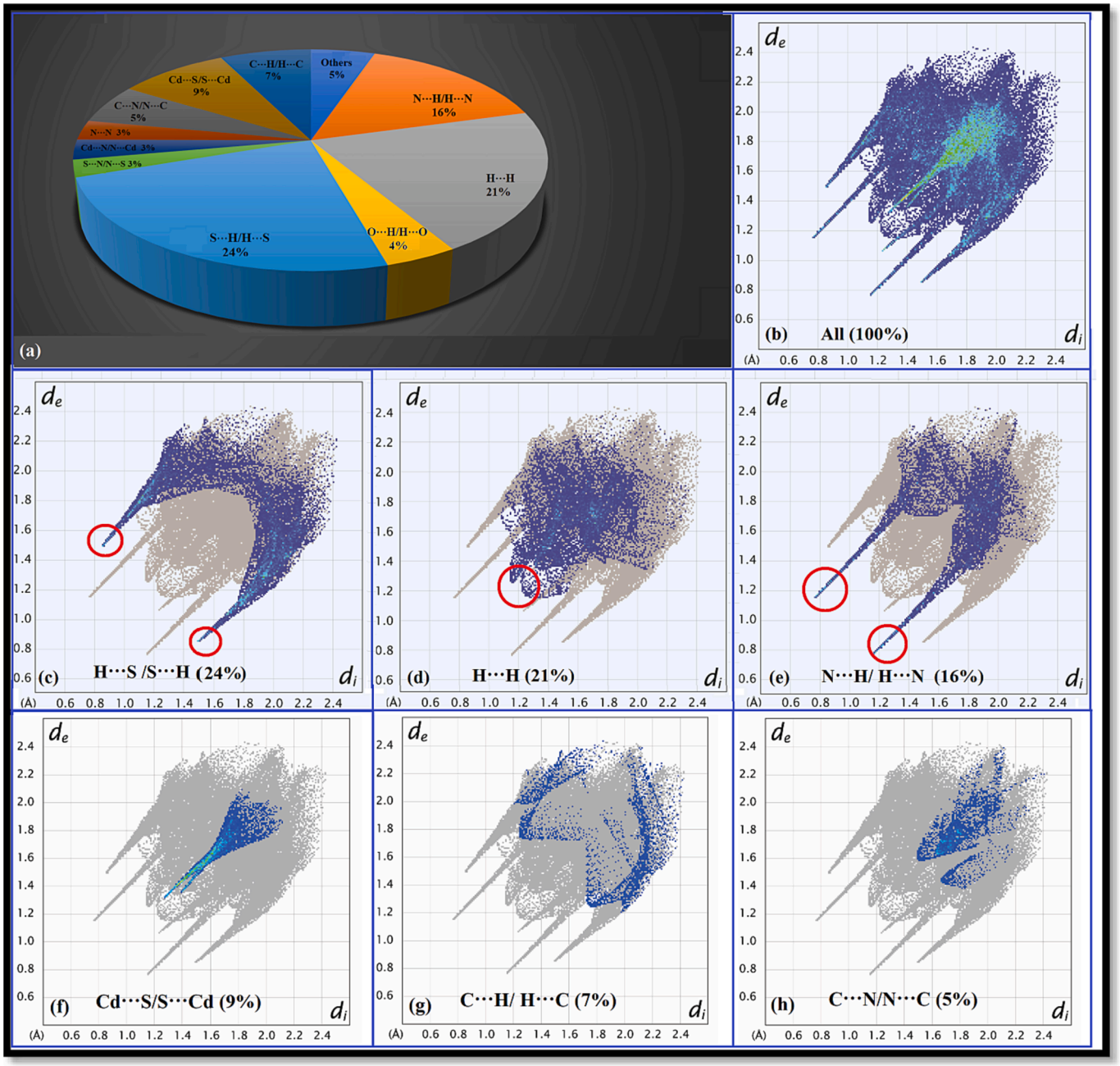

Fig. 8. Two dimensional fingerprint plots of (I) showing (a) percentage intermolecular; (b) All; (c) H···S/ S···H; (d) H···H; and (e) H···N/ N···H contacts (f) Cd···S/ S···Cd (g) C···H/ H···C (h) C···N/ N···C.

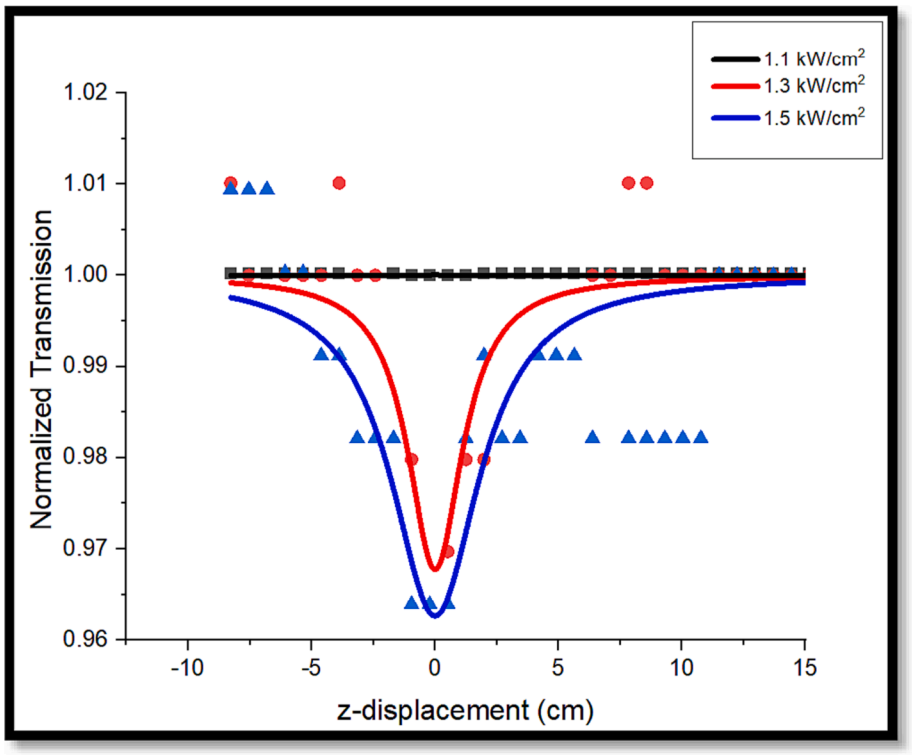

Fig. 9. Open-aperture z-scan of Cd(II)-MOFs at different intensities.

Table 3
The sign and magnitude of β and n_2 measured by fitting open z-scan and closed curve.

Cd(II)-MOFs					
Laser intensity (kW/cm^2)	β (x 10^{-4} cm^2/W)	$Im\,\chi^3$ (x 10^{-6} esu)	n_2 (x 10^{-8} cm^2/W)	$Re\,\chi^3$ (x10^{-7} esu)	χ^3 (x 10^{-6} esu)
1.1	0.0134 ± 0.15	0.0183			
1.3	5.819 ± 0.42	7.951	−8.540 ± 1.168	−7.327	7.98
1.5	6.262 ± 0.44	8.556			

same time the absorption intensity of the bands substantially grows in response to medium polarity, reaching its maximum in CH_3OH with the comparison value measured in CH_3CN. The Cd-MOF exhibits a distinct green emission at 500 nm, as evidenced by the UV absorption region observed in the CIE chromaticity diagram across a range of solvent environments.

Fluorescence spectra analysis

Room temperature Fluorescence spectra of the Cd(II)-MOFs sample with different polarities of the solvent excited based on absorbance spectra and the CIE chromocity plots of different solvent environment as is shown in Fig. 6. All the spectra exhibiting sharp UV emission peak centered at 330 nm and shoulder around 370 nm are due to the $\pi^* \rightarrow \pi$ transitions [48]. While varying the solvents with different polarity, there is no change in the fluorescence wavelength but there is slight variation in the intensity of the fluorescence spectrum. The maximum intensity was observed for the sample with CH_3CN solvent. These results suggest that PL characteristics are influenced by variations in the surrounding environment of chromophores and the solvent's interaction with functional groups. The lower intensity peaks around 580 – 680 nm corresponds to the surface defects present in the prepared samples[49].

Hirshfeld surface analysis

Hirshfeld surface (HS) analysis approaches the understanding of intermolecular interaction of molecular structure. To complete this analysis, Explorer 3.1 [50] were utilized. The HS of (I) was mapped over d_{norm} as shown in Fig. 7. Bright red spots within the molecular structure HS represent the interaction of O—H···N, O—H···S, N—H···O hydrogen bond which proven the x-ray structure analysis.

The 2D fingerprint plot (FP) for (I) showing the percentage occurrence of all types of intermolecular contacts (Fig. 8a and b). From the figure, the H···S/ S···H contact from FP shows the largest contribution of 24 %. This H···S/ S···H contact represents O—H···S intermolecular interaction of (I). While, H···H and H···N/ N···H contacts represent C—H···O and N—H···O interactions, respectively. Overall, all intermolecular interactions existed in experimental x-ray structure analysis proved and confirmed by HS analysis theoretically.

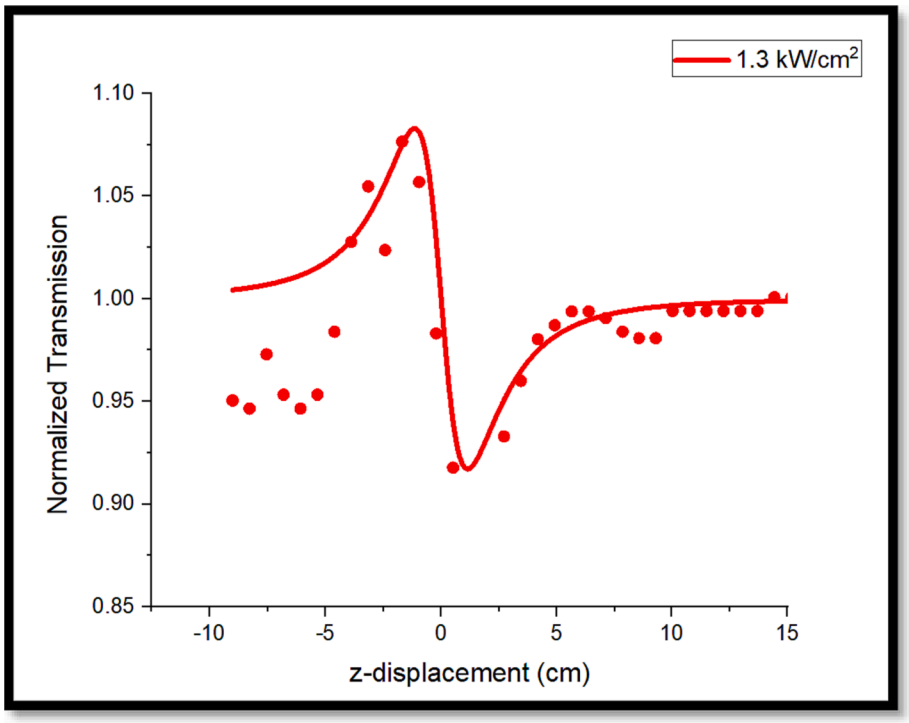

Fig. 10. Close aperture z-scan profile for Cd(II)-MOFs.

Table 4
Cd(II)-MOF nonlinear optical measurements and literature comparison of metal organic.

Name of the crystals	NLA(β) (10^{-4} cm/W)	NLR (n_2) (cm^2/W)	χ^3 (10^{-6}esu)	References
Cd(II)-MOFs	5.819 × 10^{-4}	−8.540 × 10^{-8}	7.98 × 10^{-6}	Present Work
4MBA	0.538 × 10^{-5}	−1.548 × 10^{-9}	1.075 × 10^{-7}	[35]
LTP	4.742 × 10^{-9}	1.19 × 10^{-15}	5.382 × 10^{-14}	[36]

Nonlinear optical properties

Nonlinear absorption

The open-aperture measurement (Fig. 9) was carried out at varies intensities of power laser which are 1.1, 1.3, and 1.5 KW/cm^2. Levenberg-Marquardt technique was used to compute the magnitude of in order to match the nonlinear curve. The valley and shape curve shown in Fig. 9 demonstrate suggest there is an existence of the NLA when the β coefficient is positive (Table 3) [51]. Then, suggest a significant reverse saturation absorption (RSA) at peak intensities and two-photon absorption exist. RSA illustrate the decreases in the transmittance when reach the focus point parallel to the varies intensities input power. As it reaches a bigger input of intensities laser to 1.1, 1.3, and 1.5 KW/cm^2, β was discovered increases to 0.0134, 5.819, and 6.262 x10-4 cm/W. Thus, as the intensities laser increases, more energy is received by photons to further excite at greater state. As a result of this process, the appearance of open curve existed in Fig. 9.

Nonlinear refractive

The parameter of NLR, n_2 was measured through closed aperture z-scan. The experimental results in Fig. 10 establish a good connection with the fitting line, according to a closed aperture scan. In a closed aperture curve, a peak followed by a valley feature and also negative values of n_2, −8.540 x10-8 cm^2/W, implies self-defocusing. This effect was witnessed by the changes of the employed laser irradiance passes through the chromophore [52].

Third order Susceptibilities, χ3

We have selected a few metal organics from the literature review to compare to the Cd(II)- MOFs. Interestingly, the findings (Table 3) demonstrate that Cd(II)-MOFs (χ3 = 7.98 x10- 6esu) appears to have stronger nonlinear susceptibilities when stimulated under the same circumstances as other known NLO materials (Table 4). The conjugated bonds in this molecular system are enhanced to increase the NLO property of the substance. Additionally, the existence of strong electron-donating and electron-accepting group also denotes a tendency to enhance the NLO characteristic [53]. As a result, the material for optical limiting appears promising due to its good NLO capabilities, as indicated in the table of data.

Optical limiting

Fig. 11 displays a graph of input fluence (kW/cm^2) vs normalized transmittance to study the optical limiting (OL) behaviour of Cd (II)-MOFs. It has been discovered that materials with greater NLA values show better OL values [54]. TPA and nonlinear scattering have an impact on Cd(II)-MOFs of OL. The laser fluence equation was used to determine the intensity of the transmitted light.

$$E(z) = 4\sqrt{ln2}E_{in}/\pi^{3/2}w(z)^2 \quad (8)$$

where w (z) denotes the beam radius and E in denotes the laser's input energy.

By increasing charge delocalization in the system and exhibiting a push–pull mechanism, the donor-hydrogen-acceptors in Cd(II)-MOFs optimally complement NLA as the optical limiting feature. Additionally, the material displays RSA and functions as an optical limiter due to a decreasing trend in transmittance with changes in input intensity (Fig. 11). Compound (I) is a strong choice for OL applications as evidenced by the optical limiting threshold value of 1094 kW/cm^2.

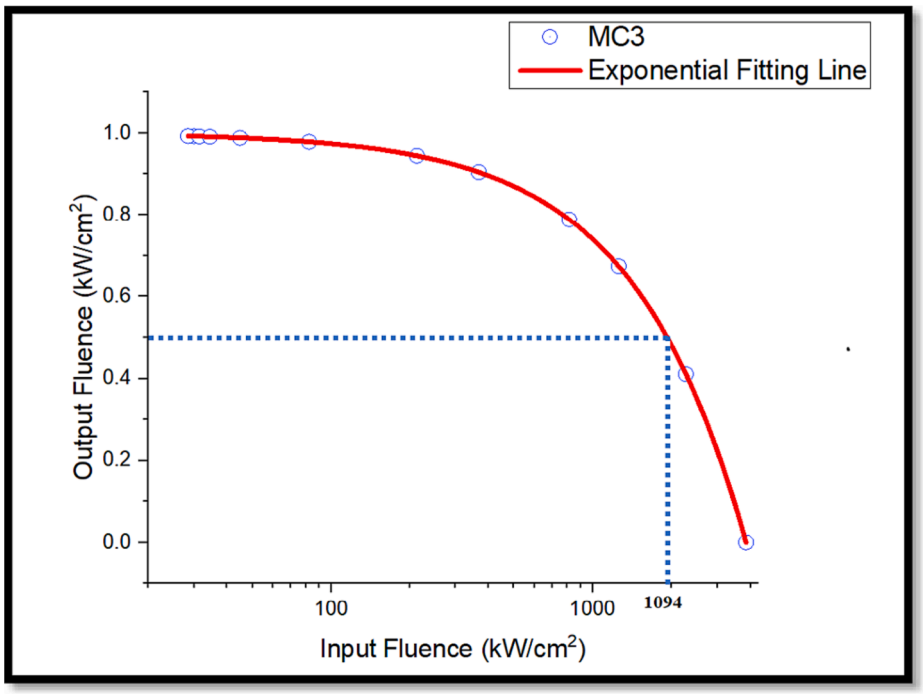

Fig. 11. Optical limiting behavior of Cd(II)-MOFs.

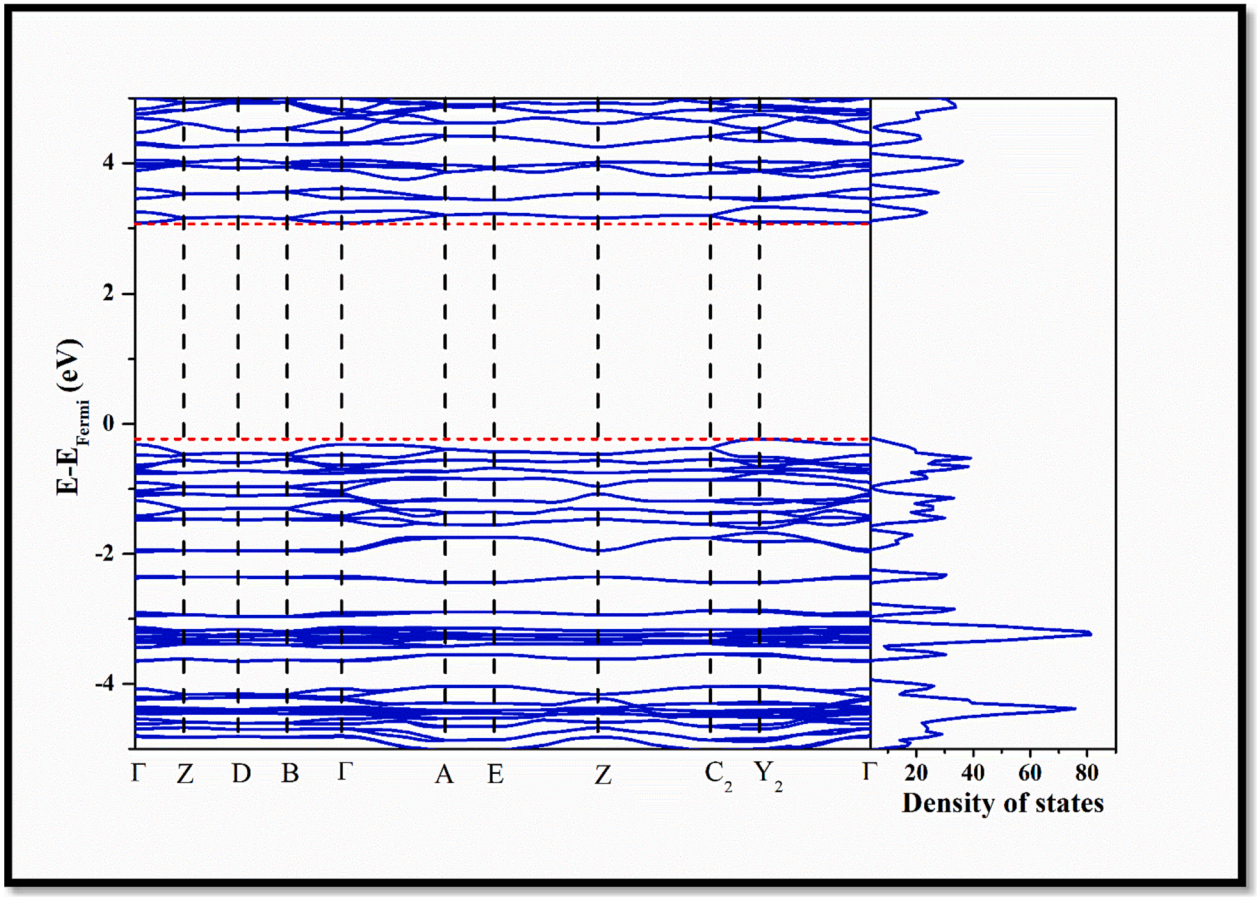

Fig. 12. Band structure and TDOS of Cd(II)-MOFs.

Band structure and TDOS

To ensure accurate results, the convergence criterion for electronic relaxation was set at 1×10^{-7} eV, and geometry optimizations were carried out until the forces acting on each atom were below 0.01 eV/Å. The Brillouin zone was sampled, with a $5 \times 5 \times 5$ k-point mesh utilized for geometrical optimization. For electronic property analysis, a denser grid of $9 \times 9 \times 9$ k-points was employed. Structural relaxations were performed, and the resulting energy-minimized configurations were utilized for further analysis. The band structure calculations were conducted along high symmetry points, including -Z-D-B–A-E-Z-C_2-Y_2- Additionally, TDOS calculations were executed using a $13 \times 13 \times 13$ k-point mesh, and the corresponding energy values were visualized using the p4vasp toolkit. In the Cd(II)-MOFs crystal, it was observed that the conduction band minima (CBM) and valence band maxima (VBM) occurred at the and Y_2 point, indicating that the material exhibits characteristics of an indirect band gap semiconductor, with a band gap measuring 3.31 eV.

Conclusion

A new poly Cadmium (II) complexes (I) metal–organic framework (MOF) crystal with potential NLO applications has been successfully synthesized. The crystal exhibits reverse saturable absorption behavior with a low optical limiting threshold of 1094 MW/cm^2, making it a promising material for optical limiting devices. Additionally, the crystal exhibits anisotropic n-channel charge carrier mobility, suggesting its potential use in other optoelectronic applications, such as field-effect transistors and solar cells.

CRediT authorship contribution statement

Anaglit Catherine Paul: Formal analysis, Investigation, Writing – original draft, Writing – review & editing. **Madhukar Hemamalini:** Funding acquisition, Investigation, Project administration, Resources, Supervision. **Mohd Mustaqim Rosli:** Writing – review & editing. **Savaridassan Jose Kavitha:** Investigation, Methodology, Writing – original draft, Writing – review & editing. **Venkatachalam Rajakannan:** Investigation, Visualization, Writing – review & editing. **V. Anbazhagan:** Formal analysis, Investigation, Methodology, Visualization, Writing – original draft, Writing – review & editing. **David Stephen Arputharaj:** Investigation, Methodology, Visualization, Writing – original draft, Writing – review & editing. **Abdullah G. Al-sehemi:** Investigation, Visualization, Writing – review & editing. **Kasthuri Balasubramani:** Writing – review & editing. **Dian Alwani Zainuri:** Investigation, Resources, Writing – original draft, Writing – review & editing. **Ibrahim Abdul Razak:** Investigation, Project administration, Resources, Supervision.

Declaration of competing interest

The authors declare that they have no known competing financial interests or personal relationships that could have appeared to influence the work reported in this paper.

Data availability

Data will be made available on request.

Acknowledgment

MH (Madhukar Hemamalini) thank the SERB-IRE for financial support – Ref. No.SIR/2022/000011. ACP (Anaglit Catherine Paul) thank the Mother Teresa Women's University, Tamil Nadu, India, for financial support DAZ (Dian Alwani Zainuri) special thanks to Universiti Sains Malaysia for the financial assistance through Short Term Grant (304/PFIZIK/6315746). ARI (Ibrahim Abdul Razak) also thank the Universiti Sains Malaysia (USM) for the research facilities. Authors acknowledge support and funding of King Khalid University through Research Center for Advanced Materials Science (RCAMS) under grant no: RCAMS/KKU/002-23.

References

[1] O.M. Yaghi, M. O'Keeffe, N.W. Ockwig, H.K. Chae, M. Eddaoudi, J. Kim, Reticular synthesis and the design of new materials, Nature. 423 (2003) 705–714, https://doi.org/10.1038/nature01650.
[2] H.-C. Zhou, J.R. Long, O.M. Yaghi, Introduction to Metal-Organic Frameworks, Chem. Rev. 112 (2012) 673–674, https://doi.org/10.1021/cr300014x.
[3] H. Furukawa, K.E. Cordova, M. O'Keeffe, O.M. Yaghi, The Chemistry and Applications of Metal-Organic Frameworks, Science. 341 (2013) 1230444, https://doi.org/10.1126/science.1230444.
[4] S. Keskin, S. Kızılel, Biomedical Applications of Metal Organic Frameworks, Ind. Eng. Chem. Res. 50 (2011) 1799–1812, https://doi.org/10.1021/ie101312k.
[5] K.K. Gangu, S. Maddila, S.B. Jonnalagadda, The pioneering role of metal–organic framework-5 in ever-growing contemporary applications – a review, RSC Adv. 12 (2022) 14282–14298, https://doi.org/10.1039/D2RA01505F.
[6] Y. He, Z. Wang, H. Wang, Z. Wang, G. Zeng, P. Xu, D. Huang, M. Chen, B. Song, H. Qin, Y. Zhao, Metal-organic framework-derived nanomaterials in environment related fields: Fundamentals, properties and applications, Coordination Chem. Rev. 429 (2021), 213618, https://doi.org/10.1016/j.ccr.2020.213618.
[7] F. Boorboor Ajdari, E. Kowsari, M. Niknam Shahrak, A. Ehsani, Z. Kiaei, H. Torkzaban, M. Ershadi, S. Kholghi Eshkalak, V. Haddadi-Asl, A. Chinnappan, S. Ramakrishna, A review on the field patents and recent developments over the application of metal organic frameworks (MOFs) in supercapacitors, Coordination Chem. Rev. 422 (2020), 213441, https://doi.org/10.1016/j.ccr.2020.213441.
[8] A. Massarotti, S. Aprile, V. Mercalli, E. Del Grosso, G. Grosa, G. Sorba, G.C. Tron, Are 1,4- and 1,5-Disubstituted 1,2,3-Triazoles Good Pharmacophoric Groups? ChemMedChem. 9 (2014) 2497–2508, https://doi.org/10.1002/cmdc.201402233.
[9] L.V. Lee, M.L. Mitchell, S.-J. Huang, V.V. Fokin, K.B. Sharpless, C.-H. Wong, A Potent and Highly Selective Inhibitor of Human α-1,3-Fucosyltransferase via Click Chemistry, J. Am. Chem. Soc. 125 (2003) 9588–9589, https://doi.org/10.1021/ja0302836.
[10] H. Zhang, X. Wang, K. Zhang, B.K. Teo, Molecular and crystal engineering of a new class of inorganic cadmium-thiocyanate polymers with host–guest complexes as organic spacers, controllers, and templates, Coordination Chem. Rev. 183 (1999) 157–195, https://doi.org/10.1016/S0010-8545(98)00270-7.
[11] M. Taniguchi, M. Shimoi, A. Ouchi, The Crystal and Molecular Structure of Bis(4-methylpyridine)bis(thiocyanato)cadmium(II) in Polymeric Form, [Cd(SCN)2(CH3C5H4N)2]n, BCSJ. 59 (1986) 2299–2302, https://doi.org/10.1246/bcsj.59.2299.
[12] M. Taniguchi, A. Ouchi, The Crystal and Molecular Structure of Bis(dibenzylamine) bis(thiocyanato)cadmium(II), Cd(SCN)2{(C6H5CH2)2NH}2, BCSJ. 60 (1987) 1192–1194, https://doi.org/10.1246/bcsj.60.1192.
[13] M. Taniguchi, Y. Sugita, A. Ouchi, The Crystal and Molecular Structures of Bis(2-methylpyridine)-, and Bis(3-methylpyridine)bis(thiocyanato)cadmium(II) in Polymeric Forms, [Cd(SCN)2(CH3C5H4N)2]n, BCSJ. 60 (1987) 1321–1326, https://doi.org/10.1246/bcsj.60.1321.
[14] V. Chenskaya, A.V. Virovets, S.A. Gromilov, N.V. Podberezskaya, T.G. Cherkasova, Synthesis and crystal structure of scandium(III) and cadmium(II) thiocyanato complexes with dimethylsulfoxide, Inorganic Chemistry Communications. 3 (2000) 482–485, https://doi.org/10.1016/S1387-7003(00)00110-6.
[15] M.A.S. Goher, F.A. Mautner, M.A.M. Abu-Youssef, A.K. Hafez, A.-M.-A. Badr, C. Gspan, Structural characterization of one-, two-, and three-dimensional polymeric complexes assembled by cadmium(II) pseudohalides and some pyridine ligands via covalent bonds and hydrogen bonds, Polyhedron. 22 (2003) 3137–3143, https://doi.org/10.1016/S0277-5387(03)00457-1.
[16] M. Julve, M. Verdaguer, G. De Munno, J.A. Real, G. Bruno, Synthesis, crystal structure, and magnetic properties of (.mu.-bipyrimidine)(cyanato)copper(II) and -(thiocyanato)copper(II) complexes, Inorg. Chem. 32 (1993) 795–802, https://doi.org/10.1021/ic00058a008.
[17] J.-C. Liu, J.-S. Guo, X.-Z. Huang, You, Different Oxidation States of Copper(I, I/II, II) Thiocyanate Complexes Containing 1,2,4-Triazole as a Bridging Ligand: Syntheses, Crystal Structures, and Magnetic Properties of 2-D Polymer CuI(admtrz)SCN, Linear Trinuclear [CuI2CuII(admtrz)6(SCN)2](ClO4)2, and Triangular Trinuclear [CuII3(admtrz)4(SCN)3(μ3-OH)(H2O)](ClO4)2·H2O (admtrz = 4-Amino-3,5-dimethyl-1,2,4-triazole), Inorg. Chem. 42 (2003) 235–243, https://doi.org/10.1021/ic0258173.
[18] M.G. Barandika, M.L. Hernández-Pino, M.K. Urtiaga, R. Cortés, L. Lezama, M. I. Arriortua, T. Rojo, Solvent control in the synthesis of [Mn(NCS)2(bpe)2(H2O)2] and [Mn(NCS)2(bpe)1.5(CH3OH)]n (bpe = 1,2-bis(4-pyridyl)ethene): structural analysis and magnetic properties, J. Chem. Soc., Dalton Trans. (2000) 1469–1473, https://doi.org/10.1039/B000808G.
[19] C.-X. Ren, H.-L. Zhu, G. Yang, X.-M. Chen, Syntheses and crystal structures of five two-dimensional networks constructed from staircase-like silver(I) thiocyanate chains and bridging polyamines, J. Chem. Soc., Dalton Trans. (2001) 85–90, https://doi.org/10.1039/B007665L.
[20] L. Cavalca, M. Nardelli, G. Fava, The crystal structure of bisbiuret-cadmium chloride, Acta Cryst. 13 (1960) 594–600, https://doi.org/10.1107/S0365110X60001424.

[21] D.-J. Li, Z.-G. Gu, J. Zhang, Auto-controlled fabrication of a metal-porphyrin framework thin film with tunable optical limiting effects, accessed November 10, 2023, Chem. Science. 11 (2020) 1935–1942, https://pubs.rsc.org/en/content/articlehtml/2020/sc/c9sc05881h.
[22] R. Medishetty, J.K. Zaręba, D. Mayer, M. Samoć, R.A. Fischer, Nonlinear optical properties, upconversion and lasing in metal–organic frameworks, Chem. Soc. Rev. 46 (2017) 4976–5004, https://doi.org/10.1039/C7CS00162B.
[23] D.M.A.S. Dissanayake, M.P. Cifuentes, M.G. Humphrey, Optical limiting properties of (reduced) graphene oxide covalently functionalized by coordination complexes, Coordination Chem. Rev. 375 (2018) 489–513, https://doi.org/10.1016/j.ccr.2018.05.003.
[24] B. Apex, SAINT, and SADABS, Bruker AXS Inc, Madison, WI, USA, 2009.
[25] C.B. Hübschle, G.M. Sheldrick, B. Dittrich, ShelXle : a Qt graphical user interface for SHELXL, J Appl Crystallogr. 44 (2011) 1281–1284, https://doi.org/10.1107/S0021889811043202.
[26] G.M. Sheldrick, SHELXS97 and SHELXL97, University of Göttingen, Germany, 1997, Google Scholar There Is No Corresponding Record for This Reference. (2001).
[27] L.J. Farrugia, *WinGX* suite for small-molecule single-crystal crystallography, J Appl Crystallogr. 32 (1999) 837–838, https://doi.org/10.1107/S0021889899006020.
[28] A.L. Spek, Single-crystal structure validation with the program *PLATON*, J Appl Crystallogr. 36 (2003) 7–13, https://doi.org/10.1107/S0021889802022112.
[29] Y. Lin, CAIROTEP : ORTEPIII incorporating CAIRO for better outputs, J Appl Crystallogr. 41 (2008) 476–478, https://doi.org/10.1107/S0021889808001647.
[30] K. Ganorkar, S. Mukherjee, P. Singh, S.K. Ghosh, Stabilization of a potential anticancer thiosemicarbazone derivative in Sudlow site I of human serum albumin: In vitro spectroscopy coupled with molecular dynamics simulation, Biophysical Chemistry. 269 (2021), 106509, https://doi.org/10.1016/j.bpc.2020.106509.
[31] S.K. Alsaee, M.A. Abu Bakar, D.A. Zainuri, A.H. Anizaim, M.F. Zaini, M.M. Rosli, M. Abdullah, S. Arshad, I. Abdul Razak, Nonlinear optical properties of pyrene-based chalcone: (E)-1-(4′-bromo-[1,1′-biphenyl]-4-yl)-3-(pyren-1-yl)prop-2-en-1-one, a structure-activity study, Optical Materials. 128 (2022), 112314, https://doi.org/10.1016/j.optmat.2022.112314.
[32] D.A. Zainuri, M. Abdullah, S. Arshad, M.S.A. Aziz, G. Krishnan, H. Bakhtiar, I. A. Razak, Crystal structure, spectroscopic and third-order nonlinear optical susceptibility of linear fused ring dichloro-substituent chalcone isomers, Optical Materials. 86 (2018) 32–45, https://doi.org/10.1016/j.optmat.2018.09.032.
[33] M.S. Bahae, A.A. Said, E.W. Van Stryland, Opt. Lett. 14 (1989) 955.
[34] G. Yang, W. Wang, L. Yan, H. Lu, G. Yang, Z. Chen, Z-scan determination of the large third-order optical nonlinearity of Rh:BaTiO3 thin films deposited on MgO substrates, Optics Communications. 209 (2002) 445–449, https://doi.org/10.1016/S0030-4018(02)01676-0.
[35] G. Vinitha, A. Ramalingam, Spectral characteristics and nonlinear studies of methyl violet 2B dye in liquid and solid media, Laser Phys. 18 (2008) 37–42, https://doi.org/10.1134/S1054660X08010076.
[36] G. Kresse, J. Furthmüller, Efficiency of ab-initio total energy calculations for metals and semiconductors using a plane-wave basis set, Computational Materials Science. 6 (1996) 15–50, https://doi.org/10.1016/0927-0256(96)00008-0.
[37] G. Kresse, J. Furthmüller, Efficient iterative schemes for *ab initio* total-energy calculations using a plane-wave basis set, Phys. Rev. b. 54 (1996) 11169–11186, https://doi.org/10.1103/PhysRevB.54.11169.
[38] S. Grimme, Semiempirical GGA-type density functional constructed with a long-range dispersion correction, J Comput Chem. 27 (2006) 1787–1799, https://doi.org/10.1002/jcc.20495.
[39] J.P. Perdew, K. Burke, M. Ernzerhof, Generalized Gradient Approximation Made Simple, Phys. Rev. Lett. 77 (1996) 3865–3868, https://doi.org/10.1103/PhysRevLett.77.3865.
[40] P.E. Blöchl, Projector augmented-wave method, Phys. Rev. b. 50 (1994) 17953–17979, https://doi.org/10.1103/PhysRevB.50.17953.
[41] P.T. Muthiah, M. Hemamalini, R.J. Butcher, catena -Poly[[[diaquacadmium(II)]-di-μ-thiocyanato] bis(2-amino-4,6-dimethylpyrimidine)], Acta Crystallogr. E Struct. Rep. Online. 61 (2005) m63–m65, https://doi.org/10.1107/S1600536804031721.
[42] G. Mostafa, A. Mondal, I.R. Laskar, A.J. Welch, N. Ray, A. Chaudhuri, Three-Dimensional Network of Cadmium, Acta Crystallogr. C Cryst. Struct. Commun. 56 (2000) 146–148, https://doi.org/10.1107/S010827019901269X.
[43] Palladium(II) complexes with 1,2,4-triazole derivative & ethylene diamine as ligands, synthesis, characterization, luminesence study & crystal structure determination - ScienceDirect, (n.d.). https://www.sciencedirect.com/science/article/abs/pii/S0277538717304527 (accessed November 10, 2023).
[44] R. Kumar, P. Bhargava, A. Dvivedi, Synthesis and Characterization of A New Cadmium Complex, Cadmium [(1,10-phenanthroline)(8-hydroxyquinoline)]Cd (Phen)q, Procedia, Materials Science. 10 (2015) 37–43, https://doi.org/10.1016/j.mspro.2015.06.023.
[45] P. Ju, M. Li, H. Yang, L. Jiang, L. Xia, R. Kong, E. Zhang, F. Qu, A novel Cd-MOF with enhanced thermo-sensitivity: the rational design, synthesis and multipurpose applications, Inorg. Chem. Front. 8 (2021) 3096–3104, https://doi.org/10.1039/D1QI00198A.
[46] N. Pandey, N. Tewari, S. Pant, M.S. Mehata, Solvatochromism and estimation of ground and excited state dipole moments of 6-aminoquinoline, Spectrochimica Acta Part a: Molecular and Biomolecular Spectroscopy. 267 (2022), 120498, https://doi.org/10.1016/j.saa.2021.120498.
[47] G. Xiao, X. Fang, Y.-J. Ma, D. Yan, Multi-Mode and Dynamic Persistent Luminescence from Metal Cytosine Halides through Balancing Excited-State Proton Transfer, Advanced Science. 9 (2022) 2200992, https://doi.org/10.1002/advs.202200992.
[48] Highly Luminescent Earth-Benign Organometallic Manganese Halide Crystals with Ultrahigh Thermal Stability of Emission from 4 to 623 K - Tan - 2023 - Small - Wiley Online Library, (n.d.). https://onlinelibrary.wiley.com/doi/10.1002/smll.202205981 (accessed November 10, 2023).
[49] M. Sheik-bahae, A.A. Said, T.H. Wei, Y.Y. Wu, D.J. Hagan, M.J. Soileau, E.W. V. Stryland, Z-Scan: A Simple And Sensitive Technique For Nonlinear Refraction Measurements, in: Nonlinear Optical Properties of Materials, SPIE, 1990, pp. 41–51, https://doi.org/10.1117/12.962142.
[50] S.K. Wolff, D.J. Grimwood, J.J. McKinnon, M.J. Turner, D. Jayatilaka, M. A. Spackman, University of Western Australia, Perth, Australia, 2012.
[51] S.K. Alsaee, E. Mzwd, M.A.A. Bakar, S.A.M. Samsuri, N.M. Ahmed, M. Abdullah, I. A. Razak, S. Arshad, Comprehensive study of solvent effects on optical characteristics for novel pyrene-based chalcone compound: (E)-1-(benzo[d][1,3] dioxol-5-yl)-3-(pyren-1-yl)prop-2-en-1-one, Optik. 272 (2023), 170384, https://doi.org/10.1016/j.ijleo.2022.170384.
[52] M.I. Rosli, M. Abdullah, G. Krishnan, S.W. Harun, M.S. Aziz, Power-dependent nonlinear optical behaviours of ponceau BS chromophore at 532 nm via Z-scan technique, J. Photochem. Photobiology A: Chem. 397 (2020), 112574, https://doi.org/10.1016/j.jphotochem.2020.112574.
[53] T.H. Clara, R. Ragu, D.R. Jonathan, J.C. Prasana, Structural, optical, thermal, dielectric and Z-scan study on novel (2E)-1-(4-aminophenyl)-3-(4-benzyloxyphenyl)-prop-2-en-1-one (APBPP) chalcone crystal for nonlinear optical applications, Optical Materials. 109 (2020), 110331, https://doi.org/10.1016/j.optmat.2020.110331.
[54] S.E. Allen Moses, S. Tamilselvan, S.M. Ravi Kumar, G. Vinitha, T.A. Hegde, G. J. Shanmuga Sundar, M. Vimalan, S. Sivaraj, Crystal structure, spectroscopic, thermal, mechanical, linear optical, second order and third order nonlinear optical properties of semiorganic crystal: l-threoninium phosphate (LTP), J Mater Sci: Mater Electron. 30 (2019) 9003–9014, https://doi.org/10.1007/s10854-019-01229-9.